Polymer Vol. 37 No. 11, pp. 2113–2123, 1996

0032-3861/96/$15.00 + 0.00

On the plastic deformation of the amorphous component in semicrystalline polymers

Z. Bartczak* and A. Galeski
Centre of Molecular and Macromolecular Studies, Polish Academy of Sciences, 90-363 Lodz, Poland

and A. S. Argon and R. E. Cohen
Massachusetts Institute of Technology, Cambridge, MA 02139, USA
(Received 23 November 1993; revised 19 May 1995)

The molecular orientation of the amorphous component of semicrystalline high-density polyethylene (HDPE) induced by plane strain compression was studied by wide-angle X-ray scattering measurements utilizing the pole figure technique and separation of the scattering produced by the crystalline and amorphous components. It was found that the oriented amorphous component produced by large strain plastic deformation consists of domains of extended chain segments, closely packed in a two-dimensional pseudo-hexagonal aggregation, which are separated by less ordered regions. The deformation leads to the formation of a texture of the amorphous component which is common to the whole sample. In this texture, the direction of the chains coincides with the direction of flow, and one of the (100) pseudo-planes of the pseudo-hexagonal structure in every domain is perpendicular to the loading direction. It was suggested that the most important deformation mechanisms in the ordered amorphous component were the glide of the chain segments along their axes and the slip of the pseudo-planes of the ordered chains in the direction perpendicular to the chain axis, with resembling the crystallographic slip processes. Such a specific deformation of the amorphous layers most probably resulted from the strong constraint imposed by the slip deformation in the crystalline component to which the amorphous component is intimately connected.

(Keywords: HDPE; wide-angle X-ray scattering; pole figure technique)

INTRODUCTION

It is now well established that the plastic deformation of semicrystalline polymers involves several mechanisms of deformation of the crystalline and amorphous components[1–3]. For the amorphous component two basic modes of plastic deformation have been proposed[4,5]: interlamellar sliding (shear) believed to be the dominant mechanism of deformation of the amorphous layers, and lamellar separation which can happen in layers between specially oriented lamellae that must thicken during crystallographic shear. It is thought that from the early stages the plastic deformation of the amorphous component (at least in HDPE) proceeds primarily by shear (interlamellar sliding)—the preferred process—before any crystallographic slip in the crystalline component can start. This process results in gradual alignment of the macromolecules in an amorphous layer along the direction of the shear of that layer, i.e. parallel to the surfaces of adjacent lamellae. However, any change of orientation of macromolecules within the thin amorphous layers located between lamellar crystals is determined not only by the externally applied stresses to the sample, but is also subject to the constraints of the adjacent crystalline lamellae to which they are intimately attached across their common boundaries by numerous tie molecules and entangled loose loops. Because of these interactions, an amorphous layer in the semicrystalline polymer will not have the same structure as the same material in the bulk and, moreover, is not free to deform in the same way as an isolated unconstrained slab of the same amorphous polymer subjected to the same stresses. The presence of such constraints is likely to impose some initial order and should result in the exhaustion of the interlamellar shear as an active deformation mode at some strain level. Further deformation of the amorphous layers after exhaustion of interlamellar sliding is possible only by accommodation of the rearrangement of the crystalline component in the course of its crystallographic slip process, thus resulting in stretching (or thickening), rotation and possible fragmentation of the crystalline lamellae.

All proposed mechanisms of plastic deformation of the amorphous component are purely descriptive and give no information about the chain rearrangement within the thin amorphous region. Since the exact nature of the amorphous material in the thin layers between lamellae is not well known, the mechanism of plastic deformation in the amorphous regions is presently not well understood. Considerations treating the deformation of these thin layers as amorphous material in bulk form are only acceptable for overall operational purposes[6].

* To whom correspondence should be addressed

A promising method for studying the deformation mechanisms which are active in the amorphous component is by the monitoring of the evolution of chain orientations in this component in the course of the deformation process by using X-ray diffraction pole figures. These have been recently employed by us to study the deformation mechanisms of the crystalline component in semicrystalline linear polyethylene and nylon-6[7–9]. The method requires deconvolution of overlapping crystalline peaks and the amorphous halo, followed by construction of pole figures for each peak and the amorphous halo from the refined data obtained by the deconvolution procedure[7].

The amorphous component consists of an assembly of macromolecules in space—albeit topologically constrained by the adjacent crystalline lamellae. The X-ray scattering pattern of this assembly is given by the sum of the Fourier transforms of the electron density functions of individual molecules. The phase shifts, introduced by each molecule having a different position in space, have to be taken into account when atomic scattering factors are added to obtain a molecular transform. These phase differences allow for interference between X-rays scattered by different molecules and formation of the scattering pattern. The X-ray halo produced by an amorphous component usually contains two distinct maxima and several very subtle ones: the first noticeable maximum for the intermolecular interferences usually occurs at lower diffraction angles because of larger distances between the macromolecules and the second one for the intramolecular interferences at higher angles[10,11]. In some polymers a single notable halo is observed, which is due to either overlapping of the inter- and intramolecular scattering or too low an intensity of the intramolecular scattering.

There has been considerable divergence of views on the state of order or disorder in amorphous polymers. The present prevailing view, based on neutron diffraction experiments[12] and X-ray scattering[13] is that there is no significant order, of even short-range nature, in flexible chain amorphous polymers, such as poly(methyl methacrylate) (PMMA) or polystyrene (PS) in bulk, but that some short-range, liquid-crystal-like ordered domains exist in many stiff chain polymers[14]. Clearly, the thin layers of amorphous material in semicrystalline polymers, especially those of high crystallinity such as polyethylene, by virtue of their attachment to crystalline lamellae, must have a certain degree of internal order. When a model of packing of the neighbouring chains within the ordered domains is assumed, the interpretation of that part of the amorphous X-ray scattering pattern which results from intermolecular interference becomes straightforward. An early model that has seen considerable development is a two-dimensional close packing of clusters of macromolecular segments in a pseudo-hexagonal arrangement (bundles model)[15–17]. In this case, the amorphous component produces reflections in the 100 range. In an unoriented polymer the ordered bundles, when present, are randomly oriented in space, which results in a scattering pattern in the form of a spherically symmetrical shell of uniform intensity centred in the origin of reciprocal space. When a preferred orientation is produced, e.g. by the deformation-induced texture the scattering is more intense in some particular directions than in others. Hence, the construction of pole figures for precisely measured amorphous halo intensities and the respective half-widths may provide information about the orientation of normals to the ordered clusters of macromolecules in the (100) planes of pseudo-hexagonal packing and the size of these 'ordered' regions, respectively[7]. In the case of semicrystalline polymers, the deconvolution of overlapping crystalline peaks and the amorphous halo is necessary to separate the scattering produced by the amorphous component.

The aim of this present study was to establish the deformation behaviour and the evolution of molecular orientation in the amorphous component of semicrystalline linear polyethylene by means of the X-ray pole figure technique.

EXPERIMENTAL

High-density polyethylene (HDPE) (Petrothene LS606-00, Quantum, USI Division, Cincinnati, OH; $M_w = 55\,000$; $M_w/M_n = 4.80$; melt flow index = 9–11 g per 10 min, according to ASTM-D-1238-57T) was compression moulded in the form of 15–20 mm thick plaques from which 10 mm thick core plates were machined out and used in the deformation experiments. The plates obtained as such had an overall crystallinity of ca. 70%, with no trace of preferred crystal orientation. The detailed description of the sample preparation is given elsewhere[9]. Plane-strain compression in a channel die was chosen as the deformation mode. Channel die compression is kinematically very similar to plane strain tension, and results in uniaxial flow of the polymer in plane strain conditions. The advantage of applying this mode of deformation is that the deformation is homogeneous in the whole range of the strain and can be interrupted at any strain level to study the actual texture and/or molecular orientation. Moreover, it avoids internal cavitation and associated artifacts which are not essential for the understanding of the texture evolution process. The compression in the channel die was performed at 80°C and the deformation rate, $\dot{\epsilon}$ was $0.0025\,s^{-1}$. The details of the deformation procedure is described in our earlier paper[9]. Four samples of HDPE compressed to the permanent true strains of 0.59, 0.92, 1.14, and 1.86 (compression ratios of 1.8, 2.5, 3.13, and 6.44, respectively) were prepared.

An automated computer-controlled Rigaku wide-angle X-ray scattering (WAXS) system, consisting of a pole figure device associated with a wide-angle goniometer coupled to a rotating anode X-ray generator operating at 50 kV and 60 mA, emitting CuKα radiation (filtered electronically, and by a Ni filter), was used in this study for the X-ray measurements. No structural studies were performed until the strain recovery after the load release had ceased (at least 24 h after unloading). The diffraction data were collected in the range of 2Θ angles from 13 to 27° in 0.2° intervals, with each set for projection of the Euler angles of sample orientation with respect to the incident beam, α (polar angle) from 0 to 90° in 5° intervals, and β (azimuthal angle) measured from the transverse direction (TD) from 0 to 360° in 5° steps. The construction of complete pole figures required the connection of the X-ray data collected in both transmission and reflection modes; the connection angle, α_c, was chosen as 45°. The slit system that was used allowed for collection of the diffraction beam with a

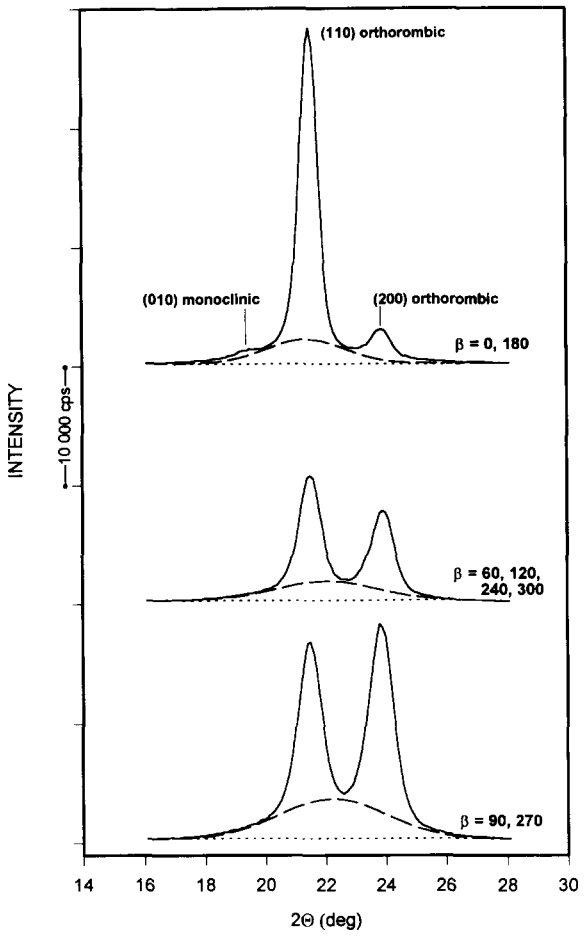

Figure 1 Examples of 2Θ scans of a HDPE sample compressed to a true strain of 1.86, recorded at various orientations of the sample in Euler space: $\alpha = 0°$, and $\beta = 0$, 60, 90, 120, 180, 240, 270, and 300°. Amorphous halo separation was performed by an elaborated fitting procedure

divergence angle of less than 0.3°. The X-ray diffraction data obtained in this way were all deconvoluted in a manner that has been described previously by us[7–9]. The fitting procedure employed in this study relies on the minimalization procedure for a least-squares expression. In this expression, the crystalline peaks, as well as the amorphous halo, were approximated by Gaussian curves. It appeared that the use of other profiles such as Lorentz or Pearson-7 produced less reasonable fits to the experimental data. The accuracy of the fitting procedure was very high and was demonstrated for compressed samples of nylon-6[7]. The representative examples of separations of the amorphous halo from the crystalline peaks in 2θ scans for $\alpha = 0°$ and various β values are presented in *Figure 1*. These scans represent the following situations: one large and one small crystalline peak on the rather small amorphous halo, two crystalline peaks of almost equal intensity on the rather small amorphous halo, and two large crystalline peaks on the large amorphous scattering. In all cases the 110 and 200 crystalline peaks do not overlap and both sit on the top of a broad amorphous halo. The 010 reflection from the monoclinic phase is seen only at $\beta = 0$ and 180°, and is very small. Thus we decided not to interpret the data for the monoclinic phase. From *Figure 1* it is seen that the amorphous scattering can be separated clearly, and with a good accuracy, from the crystalline peaks. It is unlikely that any remnant of the crystalline scattering is included in the amorphous halo. Additional confirmation of the correctness of the deconvolution procedure is provided by the density evaluation: on the basis of the deconvoluted X-ray scattering data the amount of the respective components and the density of the sample were calculated. For all samples investigated the difference between the calculated density and that measured in a gradient column did not exceed 0.1% of the measured value for samples containing one crystalline form and 0.8% for those containing two crystalline modifications. The total deconvoluted intensity, half-peak width and position of the scattering maximum data for the amorphous halo obtained from fitting were used for the construction of the pole figures presented in this report. The appropriate corrections for background scattering, Lorentz-polarization, and sample absorption were applied in the course of the deconvolution and pole figure construction procedures. The final plots of pole figures were generated by the POD program, a part of the popLA package (Los Alamos National Laboratory, Los Alamos, NM). Stereographic projection was used in the presentation of the pole figures as it emphasizes the orientations perpendicular to the flow direction, i.e. those regions of the pole figures where the concentration of normals to the (100) planes of the pseudo-hexagonal packing was expected. All the intensities of the pole figures were plotted in absolute form and no standard sample was used for reference in normalization.

RESULTS AND DISCUSSION

From the results of the X-ray diffraction measurements and the peak deconvolution procedure applied to the raw experimental data, information concerning the amorphous scattering in the whole range of directions within the sample was obtained for four specimens deformed by plane-strain compression to the following permanent true strains, i.e. 0.59, 0.92, 1.14 and 1.86. For every specimen and each pair of Euler angles (α and β) the three parameters which completely describe the amorphous scattering were determined, namely the integral intensity of scattering (i.e. the total diffracted intensity in the amorphous halo), the half-width of the halo (defined as the full width at half of the maximum) and the position of the halo (i.e. the diffraction angle at which the maximum of the amorphous halo was observed).

Figures 2a–d show the pole figures of the integral intensity of the deconvoluted X-ray amorphous halo of the deformed HDPE samples. These figures may be interpreted as the pole figures of the (100) pseudo-planes if the pseudo-hexagonal close-packing model is assumed. In *Figure 2a* it is seen that at the true strain of 0.59 concentrations of a higher intensity of the amorphous halo start to develop along two diffuse arcs, placed on the great circles inclined at ca. ±62° away from the flow direction (FD) towards the loading direction (LD). Along these arcs two maxima, not yet very distinct, can be observed. At the same time the intensity of scattering for a polar angle α close to 0° (i.e. the flow direction) decreases markedly when compared to an unoriented specimen. Similar features can be found in the pole figures plotted for the specimens deformed to true strains of 0.92 and 1.14, as shown in *Figures 2b* and *2c*, respectively. The

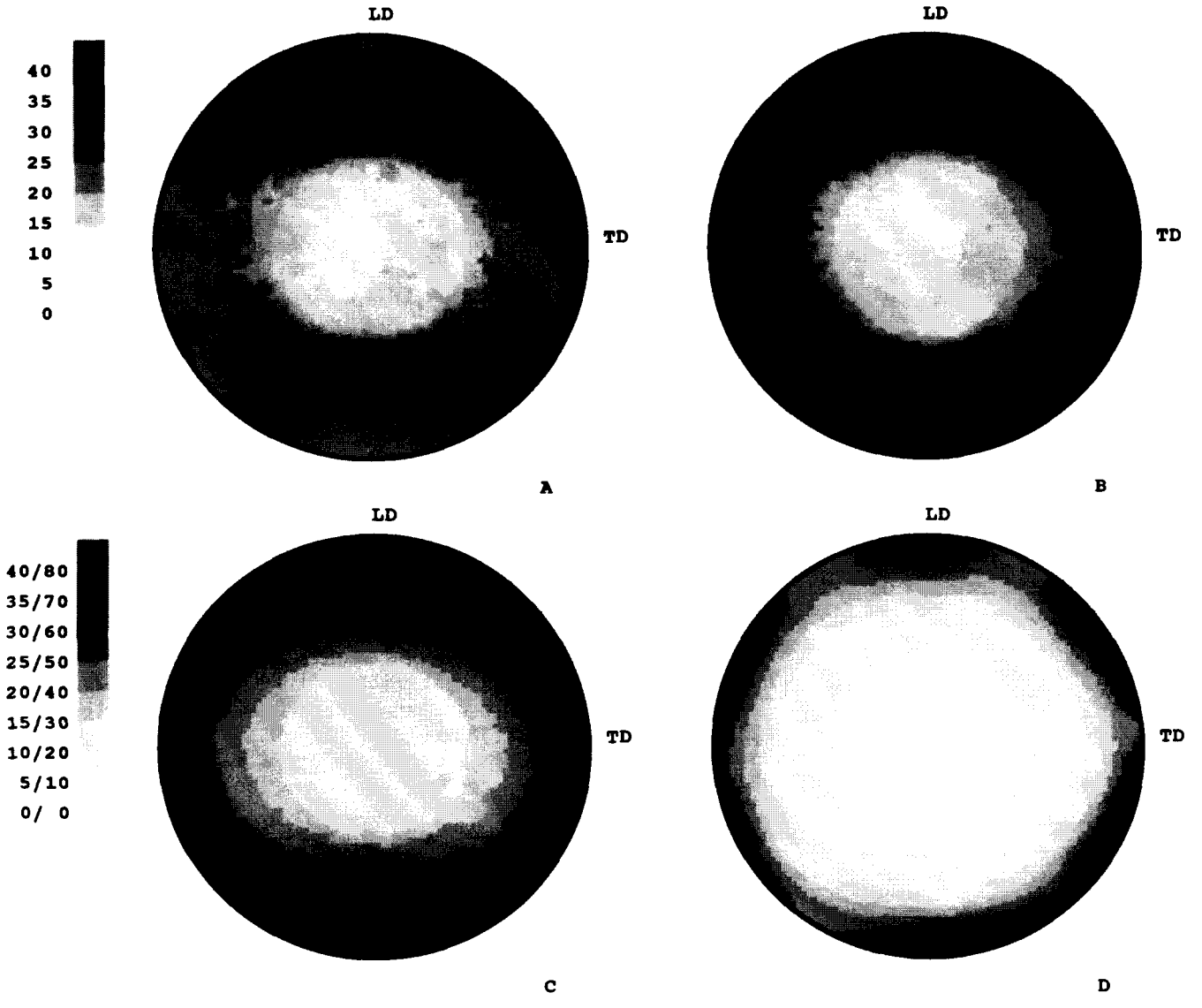

Figure 2 The integrated intensity pole figures (in stereographic projection) for HDPE samples deformed to true strain values: (a) 0.59; (b) 0.92; (c) 1.14; (d) 1.86. The loading direction and transverse direction are indicated on the figures by LD and TD, respectively; the flow direction is in the centre and perpendicular to the projection plane

angle of inclination of the arcs of high intensity increases to 68° for $\epsilon = 0.92$, and further to 72° for $\epsilon = 1.14$. It is also seen that along the high intensity arcs new local maxima develop. Closer examination of *Figure 2c* indicates the presence of three maxima for each orientation arc. Both the average intensity of scattering along the arcs and the relative height of the maxima increase with increasing strain. With a further increase in strain the angle between the flow direction and the arcs of high intensity increase further and finally, at a strain of 1.86 this angle reaches 90°, so that a single full circle placed on the perimeter of the pole figure can be observed, as is clear from *Figure 2d*. Along that circle six local maxima are now clearly seen. The azimuthal distance between each pair of maxima is 60°, and the pole figure exhibits a hexagonal symmetry, with the flow direction being a sixfold symmetry axis. The intensity at the maxima is more than one order of magnitude higher than the scattering for $\alpha = 0°$ (FD) and nearly twice as high as the intensity in six local minima located between the maxima on the circumference of the pole figure.

Figures 3a–3d show the stereographic projection maps of the half-widths of the amorphous halo as a function of the Euler angles (α and β) in the sample, plotted for the same deformed specimens (true strains of 0.59, 0.92, 1.14, and 1.86, respectively) and in the same way as the pole figures of the integral intensity presented in *Figure 2*. This method of data presentation enables an analysis of the half-width data, along with the corresponding intensity of the pole figures. These half-width 'pole figures' demonstrate that the amorphous halo from the early deformation stages is considerably wider when examined along the flow direction ($\alpha = 0°$), but sharpens continuously with increasing strain when observed along the transverse direction (TD) ($\alpha = 90°$ and $\beta = 0°$). The amorphous halo for α and β near 90° (LD) is relatively broad at initial and intermediate stages of deformation but sharpens markedly for the specimen strained to 1.86, for which the half-width of the halo for LD ($\alpha, \beta = 90°$) is practically the same as that for TD ($\alpha = 90°$, $\beta = 0°$).

A third parameter which is useful for the description of the amorphous scattering is the diffraction angle, $2\Theta_{max}$,

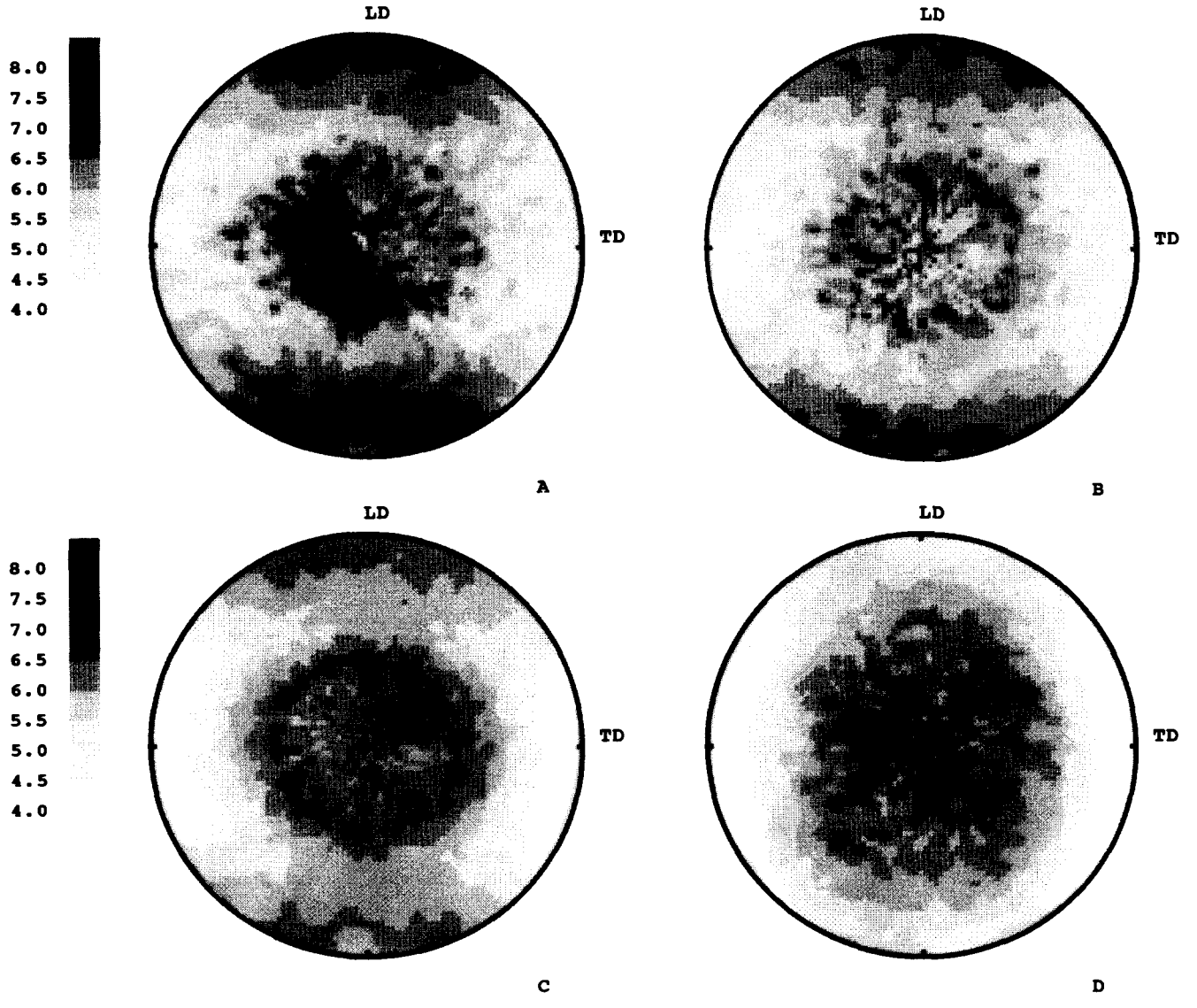

Figure 3 The stereographic projections of the full widths at half maximum of the amorphous halo for HDPE samples deformed to true strain values: (a) 0.59; (b) 0.92; (c) 1.14; (d) 1.86. The loading direction and transverse direction are indicated on the figures by LD and TD, respectively; the flow direction is in the centre and perpendicular to the projection plane. Note that the brighter areas of the maps are related to the narrower halo

at which the maximum intensity of the amorphous halo was observed. The plots of the position of this maximum as a function of orientation in the sample are shown in *Figures 4a–4d*. In a similar way to the integral intensity and the half-width maps shown in the previous figures these are also plotted in stereographic projection. *Figures 4a–4d* show that the position of the maximum is not constant as it was in an unoriented sample (for which the best-fit value of $2\Theta = 20.7°$ was obtained) but varies over the range of $2\Theta_{max}$ from ~20.0 to 22.2° depending on the direction within the sample and on the imposed strain. Starting from low strain ($\epsilon = 0.59$, *Figure 4a*) the position of $2\Theta_{max}$ as observed for $\alpha = 0°$ (FD) moves towards lower angles than observed in the unoriented sample and continues to do so with further increases in strain. Finally, at a strain of 1.86 it shifts slightly below $2\Theta = 20°$. For the same strain range ($\epsilon = 0.59$–1.14, see *Figures 4a–4c*) for directions in the specimen in the area of LD the angle of maximum amorphous scattering moves towards higher values of $2\Theta_{max}$. Moreover, an outline of two diffuse arcs of relatively high $2\Theta_{max}$ values can also be recognized. The features of these arcs are similar to previously reported arcs of high scattering intensities (cf. *Figure 2*)—they tilt gradually away from the flow direction with increasing strain. At a true strain of 1.86 they are located in the plane perpendicular to the flow direction. The highest value of the maximum diffraction angle, $2\Theta_{max} \sim 22.2°$, can be found on these arcs in the direction of loading.

As pointed out above, an amorphous component is not completely disordered but could contain short-range ordered domains in its initial unoriented state. When oriented through large strain deformation longer-range order usually develops. The verifications for such a possibility are provided, e.g. by a comparison of the measured densities with those expected for a random model[18], or by an observation of the position of the X-ray amorphous halo, shifted towards higher angles than expected from an extrapolation of the melt data to lower temperatures[19]. Both results indicate a smaller average intermolecular distance than that expected for completely disordered amorphous material, thus

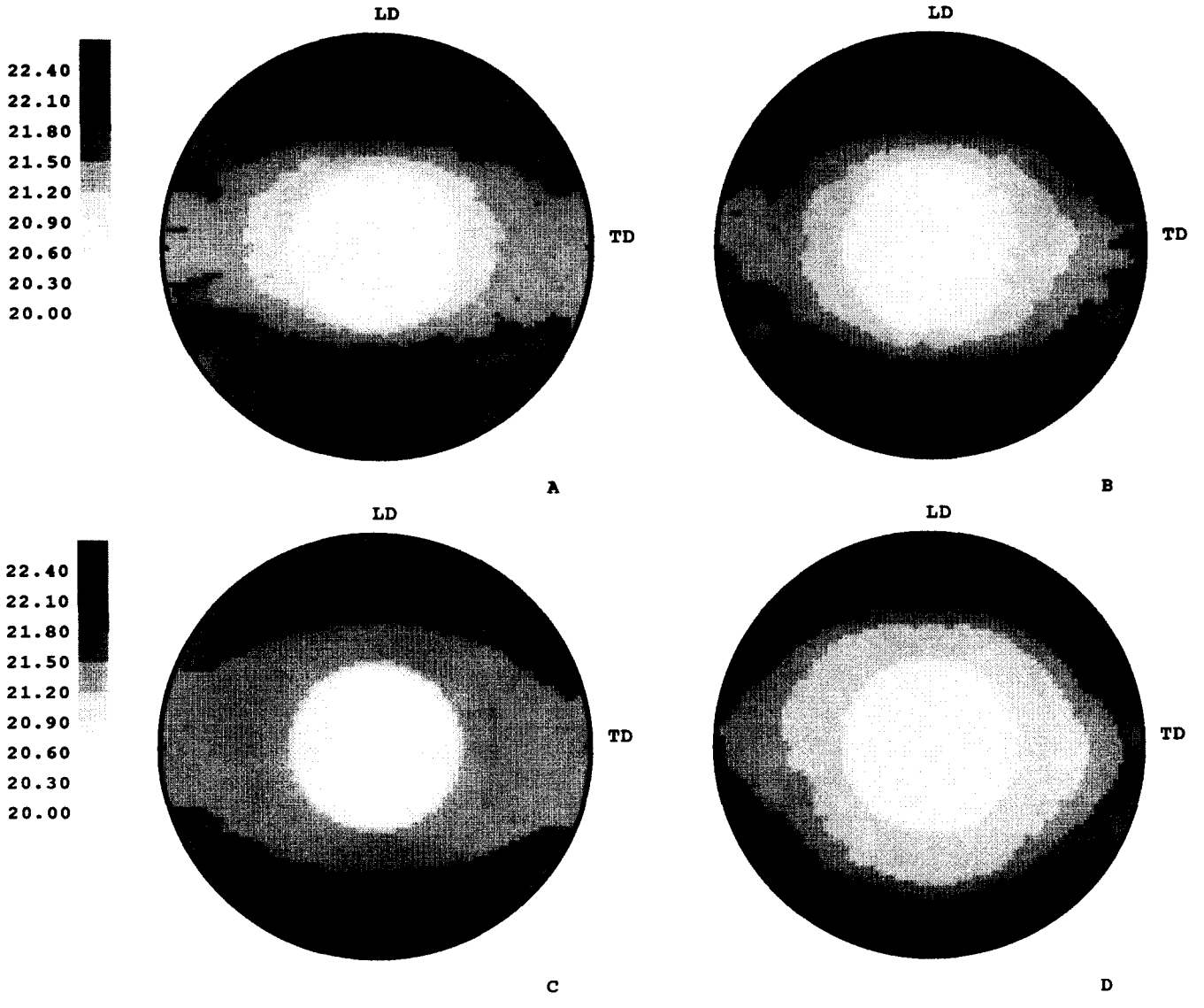

Figure 4 The stereographic projection maps of the angular position of the amorphous halo for HDPE samples deformed to true strain values: (a) 0.59; (b) 0.92; (c) 1.14; (d) 1.86. The loading direction and transverse direction are indicated in the figures by LD and TD, respectively; the flow direction is in the centre and perpendicular to the projection plane

suggesting some degree of ordering. It is believed that the amorphous component in a semicrystalline polymer, although macroscopically isotropic, can consist of micro- or submicrodomains with some, i.e. considerable, degree of internal order. The most probable arrangement of macromolecules within these ordered domains seems to be a two-dimensional close packing of the parallel clusters of macromolecules (bundles) arranged in a two-dimensional pseudo-hexagonal form[15–17]. The ordered part of the amorphous component produces reflections in the 100 range. In each ordered domain there are three families of (100) planes, with normals to them being perpendicular to the direction of the chain axis in a domain. The angle between these normals is close to 60°. The X-ray scattering by such a single domain has the form of six reflections distributed evenly on the great circle perpendicular to the direction of the chains within the domain. These reflections must be much broader than any crystalline diffraction peak because the ordering of macromolecules in a domain must be much poorer than for any crystal and the size of the domain is rather small. In an unoriented semicrystalline polymer the ordered amorphous microdomains should be oriented randomly in space. Thus, the scattering pattern assumes the form of a spherical shell of uniform intensity (the respective two-dimensional scattering pattern is in the form of a ring unrelated to the orientation of the sample with respect to the incident X-ray beam). The corresponding pole figure constructed for the intensity of the amorphous halo is then completely homogeneous. However, when a preferred orientation is produced in the sample, e.g. by plastic deformation, the X-ray scattering is no longer uniform and is usually more intense in some particular directions than in others. The lowest scattered intensity is in the direction of the preferred orientation of the molecular axis. The shape of the pole figure should depend, of course, on the method of deformation and the degree of orientation of the sample.

The amorphous halo observed for polyethylene near $2\Theta = 20°$ is most probably produced entirely by intermolecular interferences[20]. Assuming a bundle model

with pseudo-hexagonal close packing, one can easily interpret the shape of the pole figure obtained for the integral intensity of the amorphous halo of the HDPE sample deformed to the maximum true strain of 1.86 (*Figure 2d*). The concentration of high scattered intensity on the perimeter of the pole figure clearly indicates that the direction of the molecular axis is parallel to the flow direction. The presence of the distinct maxima on the perimeter and their sixfold symmetry supports the hypothesis of hexagonal close packing of macromolecules in this highly oriented sample, with the maxima undoubtedly being produced by diffraction from the (100) planes of the hexagonal aggregation. The most surprising fact is that the ordered domains (bundles) are oriented in the same manner with respect to the LD (or TD) as the crystalline component. The reported result indicates that the majority of the amorphous component gained the same orientation in the course of the deformation process, in spite of the very complex topology and discontinuity of this component in the semicrystalline polymer where the amorphous layers are separated from each other by crystalline lamellae. The above result was at first quite unexpected since it might be expected that the orientation of the amorphous phase merely resembles a fibre texture with only the molecular axis orientation being well defined and having no lateral correlation of the orientation of the domains around the flow direction.

An understanding of the origin of the shape of the pole figure for the sample deformed to the highest strain ($\epsilon = 1.86$) makes the interpretation of the pole figures easier for those specimens which were deformed to smaller strains ($\epsilon = 0.59$, 0.92, and 1.14). The pole figures in *Figures 2a–2c* for these specimens could be interpreted as intermediate states between an initial state of disorder of hexagonally packed domains that are in the course of deformation to a final, almost fully aligned state. In all of these figures an outline of the same type of texture can be recognized. This texture consists of two texture elements, with each of the same hexagonal-type symmetry as the single texture observed in the sample of strain of 1.86, but being tilted symmetrically on both sides of the flow direction towards the loading direction in the LD–FD plane. With increasing strain this tilt angle gradually decreases down to 0° for $\epsilon = 1.86$. For this strain both texture elements merge to form a single texture which is centred in the flow direction. At low strain, i.e. $\epsilon = 0.59$ (*Figure 2a*), not all of the intensity maxima that are expected for hexagonal packing are yet fully developed. One can identify only contours of the two strongest of these. However, the remaining maxima become visible at higher strains (see *Figures 2b* and *2c* for $\epsilon = 0.92$ and 1.14, respectively), which supports the proposed texture interpretation. All of the maxima formed have the same position along the great circle (in Euler space, not in the pole figure) which is perpendicular to the texture axis, and independent of the actual strain. This indicates that both texture elements of the amorphous component once formed, rotate with their reference axes (molecular axes, ***m***) towards the FD with increasing strain.

The evolution of the molecular orientation of the amorphous component during plane-strain compression follows to some extent the pattern which is characteristic of the crystalline component[9]. Both of the components form two populations of anisotropic units (bundles and crystals, respectively) oriented with their molecular axes, ***m*** and ***c***, symmetrically with respect to the flow direction. These molecular axes rotate towards the FD with increasing strain and finally align along this direction for very large strain. This could suggest that the interlamellar shear responsible for orientation of the amorphous phase is realized on the molecular level by a mechanism which may be quite similar to crystallographic slip, i.e. the main deformation mechanism of the crystalline component[1–3,9]. At any strain the angle between ***m*** and the FD is a few degrees smaller than the angle between ***c*** and the FD at the same strain (see *Table 1*), which indicates a somewhat faster rotation of the amorphous domains than the crystals. This is probably a result of the lower plastic resistance of the amorphous component than the crystalline component (less than 5 MPa for the former vs. 7.2 MPa, for the latter[9,21]), which causes the deformation of the amorphous component to start at an earlier stage in the deformation process. Thus, it is more advanced than the deformation of the crystals at a given strain, especially at the initial and intermediate stages of deformation. Such a conclusion is strongly supported by the results of computer simulations of the plastic deformation of semicrystalline linear polyethylene[6].

Table 1 Values of the angles between the flow direction and the directions of the molecular axes for the crystalline and amorphous phases

True strain	∢(***m***, FD) (°)	∢(***c***, FD) (°)
0.59	28	32
0.92	22	24
1.14	18	20.5
1.86	0	0

The width of the amorphous halo in terms of the close packing model is influenced by several broadening effects resulting generally from the irregular packing within the domains, i.e. from the finite size of these domains and from scattering by the numerous segments which are outside of the ordered bundles. In the first approximation, the half-width of the amorphous halo, measured at a given direction in the sample, can be simply interpreted as a qualitative measure of the average size of these ordered domains which are oriented with their molecular axes, ***m***, perpendicular to that direction. Similar to the diffraction from a crystal lattice with width of the reflection produced by the diffraction from the (100) planes of the pseudo-hexagonal aggregation should be reciprocally dependent on the size of the ordered regions in the direction perpendicular to that plane. That direction is always perpendicular to the chain direction, ***c***, in the domain, and thus the half-width data can provide qualitative information about the lateral sizes of the ordered close packed regions in the amorphous component. Such an interpretation is, of course, a very rough simplification, and does not account for possible variations of the internal order of the clusters and/or the internal stress build-up during the deformation process, which can influence to a large extent the width of the amorphous reflection. The separation of the effects of the above factors is possible in principle, e.g. on the basis of Hoseman's paracrystal model[22]; however, the result would be quite uncertain.

Figures 2a–2d show that in the samples of deformed polyethylene the half-width of the amorphous halo varies over a relatively broad angular range of 3.6–7.5°, depending on the direction within the sample. This range of variation was common for all of the deformed samples that were investigated. In the case of undeformed polyethylene the half-width of the amorphous halo was determined as being close to 5°. From *Figure 2* it is seen that for every strain there is a significant broadening of the amorphous halo in the direction of the FD as compared to the unoriented sample. Such broadening indicates either a decrease of the lateral size of these ordered domains, which are oriented with their molecular axes roughly perpendicular to the FD, or alternatively a substantial decrease of their internal order. In contrast, the domains which are oriented with their molecular axes around the FD generally give rise to a narrower halo, which indicates that the lateral sizes are larger than in other domain populations or in an undeformed polymer. Again, an alternative explanation of an improvement of the internal order within domains is possible. On the other hand, the half-width of the profile of scattering produced by these planes is still relatively large, i.e. close to 3.6°, which is much wider than the width of the diffraction peak produced by any crystal plane. This means, that the average lateral size of the highly ordered regions of the amorphous component in deformed polyethylene samples, albeit larger than in unoriented material, is still much smaller than the crystallites. The alternative interpretation is again that the perfection of ordering in domains increases. The conclusion can be drawn that the amorphous component does not transform its morphology substantially during the deformation process; the ordered domains are aligned in the flow direction and possibly grow in diameter to some extent and/or improve their internal order, but most probably do not coalesce to form considerably larger ordered regions.

The analysis of the data of the position of the amorphous halo, presented in *Figure 4*, can provide additional useful information concerning the structure of the amorphous regions. The position of the halo is related to the average interchain distance in the amorphous component. Considering the structure of this component as a two-dimensional close packed pseudo-hexagonal structure, the position of the halo is determined by the (100) interplanar distance by the use of Bragg's law. If we consider the pattern of *Figure 4* as representing the postulated structure, the points O, A, B, C, D, E, and F are the projections of the polymer chains, OE ($= l$) is the typical interchain distance and OH ($= d_{Bragg}$) is the distance between the (100) planes. The volume occupied by a monomeric unit in such a hexagonal structure can be calculated, while, on the other hand, the same volume of the monomeric unit can be obtained from the density. Combining these two formulae for the volume of the unit by using Bragg's law, one can estimate the density of the amorphous component for a given position of the amorphous halo. Such an estimation performed for unoriented polyethylene, for which we measured $2\Theta_{max} = 20.7°$ at room temperature gives an estimate of the average interchain distance, l, of 4.955 Å and a density of the amorphous component, ρ, of 0.860 g cm^{-3}, which is very close to the value of 0.855 g cm^{-3} reported for amorphous polyethylene in the literature[23]. This result strongly supports the hypothesis that the pseudo-hexagonal close packing of the chain segments in the amorphous component is possibly already present in the unoriented material.

Figure 4 shows that the position of the amorphous halo in deformed samples depends on the strain and direction in the sample. For $\epsilon = 1.86$ (see *Figure 4d*) the amorphous halo in the FD, i.e. originating from those chain segments which are oriented perpendicular to the FD, is centred slightly below $2\Theta = 20°$. The respective interchain distance is 5.14 Å. On the contrary, the halo as observed on the perimeter of the map, i.e. produced by the interferences of the chain segments oriented along the FD, have a relatively high position, namely up to $2\Theta_{max} = 22.2°$. The interchain distance associated with that position can be estimated as 4.66 Å. This value is only a little larger than the interchain distances in the crystalline component (4.46 Å in the (110) planes of orthorhombic polyethylene). The density of the amorphous component estimated for such an orientation is very high, i.e. $\rho = 0.96$ g cm^{-3}, which is also very close to the density of the crystalline component, namely $\rho = 1.0$ g cm^{-3} (ref. 23). These results suggest a very high degree of ordering of the amorphous chains oriented along the FD. A more detailed examination of the data presented in *Figure 4d* reveals additionally, that for chains oriented along the FD there is a dependence of the (100) interplanar and interchain distances on the direction in the LD–TD plane. The interplanar distances calculated for various directions correspond to the pseudo-hexagonal structure based on a slightly distorted hexagon with an EOF angle (see *Figure 5*) close to 59.4° instead of 60°, as expected for a regular hexagonal structure. The orientation of this structure is that OH is parallel to the loading direction and OB is parallel to the transverse direction. The very high degree of order of the chains oriented along the FD, as suggested by the position of the halo, leads to the question as to whether the ordering is only two-dimensional as postulated initially, or is there also some detectable ordering in a third direction, along the chain axis? If so, one should observe an additional scattering maximum produced by the ordered amorphous component in the direction of the FD. Such a maximum should be positioned near $2\Theta = 35$ or 74° (= 2.54 or 1.27 Å, respectively, which are the most probable periods of such ordering, and equal to

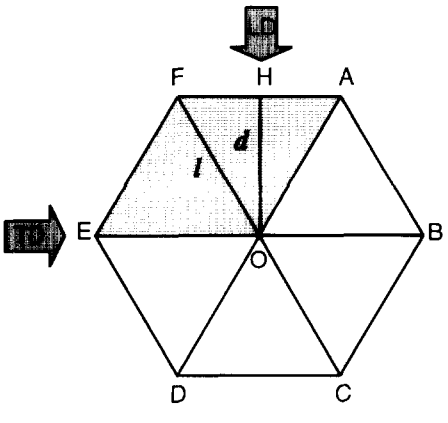

Figure 5 Projection of the postulated close packing structure of the ordered domain on the plane perpendicular to the chain axis

the distances between the hypothetical planes perpendicular to the chain axis and including the carbon atoms). However, for these ranges of the Bragg angle we have observed in deformed samples only the high and sharp 020 and 002 peaks of the orthorhombic polyethylene crystals, with no traces of a broader, amorphous-like scattering in the background. This result indicates that the ordering along the chain within the ordered amorphous regions does not exist, or is too imperfect to be detected. Thus, the two-dimensional pseudo-hexagonal structure, with its principal hexagonal axis aligned parallel to the FD, seems to be a correct model of the ordering of the oriented amorphous component of linear polyethylene.

On the basis of the above discussion the following picture of the structure of the oriented amorphous phase in linear polyethylene can be proposed: the chains constituting the amorphous component have numerous extended fragments which are aligned parallel to the flow direction and are arranged in a two-dimensional degenerate hexagonal packing in the LD–TD plane. The hexagonally ordered extended chain segments are arranged in separate domains, (bundles), which are relatively small in size when compared with the crystallites. The orientation of the hexagonal network in every bundle is practically the same, and is common for the whole sample. The degree of ordering of the chains in the domains is very high and the average interchain distance, l, of 4.66 Å, is not far from the respective distances observed in the orthorhombic crystalline component. The oriented domains are separated from each other by almost completely disordered amorphous regions in which the average interchain distance is much higher. Most probably, all the mutual chain entanglements and other spatial defects are concentrated in these regions. Rather similar conclusions were reached by Gibson *et al.*[24] in their study of ultra-high-modulus PE, with, however, much less information on the state of the amorphous component.

The most appealing picture that emerges for both the origin of the gradually evolving hexagonal symmetry in the amorphous material reported here, and its possible role in the deformation of the entire semicrystalline HDPE can be described as follows. There is some evidence that can be interpreted that at least some of the ordered hexagonal domains exist in the melt processed interlamellar amorphous material prior to deformation[20]. These ordered domains, evidently part of the inter-crystalline tie links, are small in their lateral dimensions, have no important axial coherence and are separated by completely disordered tie links making up a topologically continuous sub-component surrounding the ordered domains. In HDPE, where the entire amorphous component exists above its glass transition temperature (T_g), neither the ordered nor the disordered sub-component parts will offer significant deformation resistance in the early stages of deformation. This is evidenced by the observation that the early stages of plastic deformation of an initially spherulitic material are made up almost entirely of interlamellar shear in which the hexagonally ordered domains must be deforming by mechanisms akin to chain slip and transverse slip on the three equivalent (100)-type planes of this material, and where the tie links of the disordered components accommodate in a more complex manner by stretching out as much as possible as the shear of the hexagonal domains demand.

When the early stages of interlamellar shear are exhausted, primarily due to the stretching out of the disordered tie links, the less easily deformable crystalline component begins to deform by chain slip and transverse slip on the (100) and (010) planes, as discussed by us earlier in considerable detail[9,21]. This dominant crystallographic slip-type deformation of the crystalline component occurs first by relatively independent ways from the amorphous component, where the latter remains attached to the crystalline lamellae and deforms only to the extent demanded by the shearing and rotating lamellae. This kinematically uncomplicated state of deformation, which proceeds uninterrupted to a true strain of approximately 1.2 in plane strain compression, has been quite successfully modelled by Lee *et al.*[6]. Over this stage of strain there is little or no mixing of the amorphous and crystalline components and their common interfaces remain distinct. At a true strain of about 1.2, a major restructuring of the entire crystalline and amorphous components occurs. Because this critical strain and the eventual true strain of 1.86, shown in *Figures 2–4* (parts d), the shearing lamellae pinch off, become fragmented, and an extensive translation of the interfaces between the amorphous and crystalline components occurs. This involves reincorporation of some amorphous tie-link segments into the crystalline component as chain defects and a corresponding rejection of some previously crystalline component into the ordered component of the amorphous material. The WAXS pole figures show that during this stage of straining a long-range coherence develops in the entire aligned molecular assembly. In this process of alignment the deformation of the crystalline component is dominant and the intimately attached amorphous component is forced to conform to the imposed deformation in several ways. First, any pre-existing hexagonally ordered domains attached to the crystallites readily transmit the principal (100)[001] chain slip operation of the orthorhombic crystallites along their (100) planes. The remaining disordered sub-component of the amorphous material is also regrouped into ordered hexagonal domains. This occurs, whenever possible, by incorporation of some tie-links into the shearing crystalline lamellae as chain packing defects. By motion along the chain, these previous tie-link segments become redistributed along the aligned molecules of the crystallites. This also serves to force the remaining disordered amorphous sub-component into the hexagonally ordered form, in registry with the orthorhombic lattice of the crystallites, and also begins to transmit the (100)[001] chain slip mode. In this manner, the hexagonally ordered amorphous component not only stretches out and aligns, but also assumes a coherent registry with the orthorhombic lattice of the crystallites, thus resulting in the alignment of the (100) planes in the orthorhombic crystals with the (100) planes of the pseudo-hexagonal domains in the amorphous component. These exchange operations between the crystalline and amorphous components make the crystallites somewhat less perfect, but the amorphous components become well aligned and coherent with the crystallites. How well this succeeds is clear from *Figure 6*, which shows that when viewed in the chain direction the orthorhombic lattice and the

hexagonal pseudo-lattice of the amorphous component show a remarkably close fit.

These envisioned processes of shear induced alignment and ordering are evidenced by a very substantial weakening of the SAXS patterns[9] and an accompanying substantial broadening of the distribution of the new long period normal to the FD of the principal molecular alignment in the samples with a true strain of 1.86. Thus, this confirms the dispersal of the defected amorphous material and the diffusion of the previously clear amorphous/crystalline interface as the long-range coherence develops. This long-range coherence of the crystalline and amorphous components into an unbroken quasi-crystal of macroscopic dimensions has been established by Schönherr *et al.*[25] by means of atomic force microscopy (AFM) on the (100) surfaces of highly oriented material which has been deformed to a true strain of 1.86, where the remarkable perfection of the material has permitted the obtaining of molecular level resolution. Such AFM observations on the (100) surfaces revealed no clearly identifiable amorphous layers over dimensions of the order of 50 nm along the chain direction (FD) (i.e. over several expected long-period dimensions). Careful scrutiny of these micrographs, however, revealed a collection of well-dispersed chain defects in the form of 'flip-overs' of two parallel chains, small amplitude, long wavelength waviness and other ill-defined short-range irregularities among the aligned molecules. This reinforces the findings of this present study rather well.

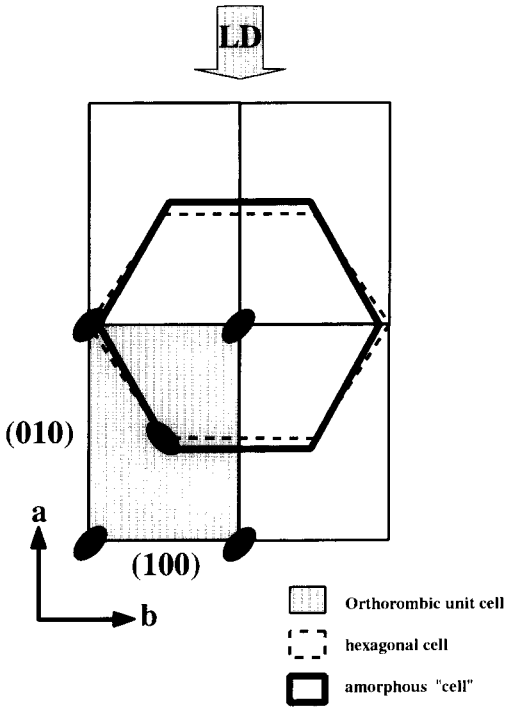

Figure 6 Schematic representations of the orthorhombic and hexagonal pseudo-lattice. The strong constraints of the crystallographic slip processes in the crystalline component results in an eventual close registry of the orthorhombic crystal structure of the crystalline component with the pseudo-hexagonal structure of the amorphous component. Four neighbouring orthorhombic unit cells of the crystalline component with a superimposed pseudohexagonal unit cell, as postulated for the oriented amorphous component, are projected on the plane perpendicular to the chain axis

CONCLUSIONS

The experimental results discussed in this paper show that the plastic deformation of semicrystalline linear polyethylene in plane strain compression induces a preferred orientation of macromolecules, not only for the crystalline component, but also for the amorphous component. The oriented amorphous component produced by large strain plastic deformation consists of domains of extended chain segments which are closely packed in a two-dimensional pseudo-hexagonal aggregation. The deformation, in plane strain compression, induces their reorientation and the formation of a texture which is common for the whole sample. In the final texture of the amorphous component the chain axes of the domains are oriented along the flow direction and one of the (100) planes of the pseudo-hexagonal structure of every domain is perpendicular to the loading direction. This comes about as a result of the strong constraint imposed by the chain-slip deformation in the orthorhombic crystalline component to which the amorphous component is intimately connected. The plastic deformation of the amorphous component proceeds mostly in the ordered domains and the deformation mechanisms involved here are, in our opinion, quite similar to the mechanisms active in the deformation of the crystalline part of the polymer. While this is a conjecture for the early stages of deformation it becomes a necessity in the final stages when long-range coherence is established. We suggest that the most important mechanisms in the ordered amorphous component are the glide of the chain segments along their axes, resembling the crystallographic chain slip active in the crystals, and the slip of such planes of the ordered chains, which resemble the crystallographic transverse slip. Both of these suggested 'slip' mechanisms act in the (100) planes of the pseudo-hexagonal structure of the ordered domains. Because of the hexagonal symmetry of the domain structure, four independent 'slip systems' can operate in each domain. This indicates that the ordered amorphous components have the same degrees of freedom and kinematic constraints as the crystalline components. Because of the higher plastic resistance of the crystalline component when compared to the amorphous component the plastic deformation localizes initially in the amorphous layers as interlamellar shear, which in turn produces relatively large local strains. When the plastic deformation of the crystallites by chain slip sets in this results in the rotation of the amorphous layers located between the lamellae. This in turn, alters the orientation of the amorphous chains. Continuation of these processes during deformation produces systematic alterations that eventually result in long-range coherence, where the degree of orientation in the amorphous and crystalline components approach each other.

ACKNOWLEDGEMENTS

The research of Z. Bartczak and A. Galeski was supported by the Polish Academy of Sciences, while that of A. S. Argon and R. E. Cohen was supported by a DARPA/URI programme under ONR Contract No. N00014-86-K-0768.

REFERENCES

1 Bowden, P. B. and Young, R. J. *J. Mater. Sci.* 1974, **9**, 2034
2 Haudin, J. M. in 'Plastic Deformation of Amorphous and Semi-Crystalline Materials' (Eds B. Escaig and C. G'Sell), Les Editions de Physique, Paris, 1982, p. 291
3 Lin, L. and Argon, A. S. *J. Mater. Sci.* 1994, **29**, 294
4 Keller, A. and Pope, D. P. *J. Mater. Sci.* 1971, **6**, 453
5 Pope, D. P. and Keller, A. *J. Polym. Sci. Polym. Phys. Edn* 1975, **13**, 533
6 Lee, B. J., Argon, A. S., Parks, D. M., Ahzi, S. and Bartczak, Z. *Polymer* 1993, **34**, 3555
7 Galeski, A., Argon, A. S. and Cohen, R. E. *Macromolecules* 1991, **24**, 3945
8 Galeski, A., Argon, A. S. and Cohen, R. E. *Macromolecules* 1991, **24**, 3953
9 Galeski, A., Bartczak, Z., Cohen, R. E. and Argon, A. S. *Macromolecules* 1992, **25**, 5705
10 Voigt-Martin, I. and Wendorff, J. H. in 'Encyclopedia of Polymer Science and Engineering' (Eds H. F. Mark, N. M. Bikales, C. G. Overberger and G. Menges), Vol. 1, 2nd Edn, Wiley, New York, 1985, p. 789
11 Windle, A. H. in 'Development in Oriented Polymers' (Ed. I. M. Ward) Applied Science, London, 1982, p. 1
12 Kirste, R. G., Kruse, W. A. and Ibel, K. *Polymer* 1975, **16**, 120
13 Mitchell, G. R. in 'Order in the Amorphous "State" of Polymers' (Eds S. E. Keinath, R. L. Miller and J. K. Rieke), Plenum, New York, 1987, p. 1
14 Russel, T. P., Brown, H. R. and Grubb, D. T. *J. Polym. Sci. Polym. Phys. Edn* 1987, **25**, 129
15 Ovchininikov, Yu. K., Markova, G. S. and Kargin, V. A. *Polym. Sci. USSR (Engl. Transl.)* 1969, **11**, 369
16 Gurato, G., Fichera, A., Grandi, F. Z., Zanetti, R. and Canal, P. *Makromol. Chem.* 1974, **175**, 953
17 Kan, S. and Seto, T. *Rep. Prog. Polym. Phys. Jpn.* 1976, **19**, 219
18 Robertson, R. E. *J. Phys. Chem.* 1965, **69**, 1575
19 McFaddin, D. C., Russel, K. E., Wu, G. and Heyding, R. D. *J. Polym. Sci. Polym. Phys. Edn* 1993, **31**, 175
20 Mitchell, G. R., Lovell, R. and Windle, A. H. *Polymer* 1982, **23**, 1273
21 Bartczak, Z., Argon, A. S. and Cohen, R. E. *Macromolecules* 1992, **25**, 5036
22 Hoseman, R. *Polymer* 1962, **3**, 349
23 Brandrup, J. and Immergut, E. H. (Eds) 'Polymer Handbook' 3rd Edn, Wiley, New York, 1989, p. V/15
24 Gibson, A. G., Davies, G. R. and Ward, I. M. *Polym.* 1978, **19**, 683
25 Schönherr, H., Vansco, G. J. and Argon, A. S. *Polymer* 1995, **36**, 2115